Statistical thermodynamics of micellar solutions

F. H. Stillinger and A. Ben-Naim[a)]

Bell Laboratories, Murray Hill, New Jersey 07974
(Received 10 October 1980; accepted 27 October 1980)

In order to study the behavior of surfactant solutions near their critical micelle concentrations (CMC's), the osmotic pressure and monomer concentration functions have been examined in the complex plane of total surfactant concentration y. By considering some simple models in detail it has been established that a locus of branch-point singularities for both functions intersects the positive real y axis at the CMC's. The proximity of the closest branch-point pair straddling the real axis is related on the one hand to mean micelle size, and on the other hand to the sharpness of the critical micelle phenomenon. A perturbation procedure has been constructed which can help to locate the physically important branch points near the positive real axis for the general ideal solution case.

I. INTRODUCTION

Aqueous solutions of micelle-forming surfactants (amphiphiles) exhibit an intriguing richness of behavior. Therefore it is hardly surprising that frequent and intense research effort has been expended to understand these systems. Furthermore that effort is justified by the importance of surfactants for topics as diverse as chemical catalysis, crude oil recovery, and membrane structure in biology.[1-3]

Considerable theoretical attention has already been devoted to developing a microscopic theory of micelle formation.[4-8] However progress has been hampered by general ignorance of the way that amphiphiles interact with one another and with the solvent, and of the distribution of micelle shapes. It has been our goal in the present work to develop a procedure which could help to infer the missing information from carefully executed experiments.

To be specific, the micelles of interest here are those that form in dilute solution, and have finite size. We exclude from consideration aggregates that are infinite in one or more dimensions. Both ionic and nonionic surfactants are considered, however.

The size range for finite micelles is rather variable. The number of molecules incorporated in the aggregates apparently can range from a few tens to several thousand.[9] The sudden appearance of micelles in the solution at the critical micelle concentration (CMC) can be viewed as an arrested form of phase separation. Because only finite numbers of surfactant molecules cluster together (rather than the essentially infinite number in a true phase separation) properties only exhibit rapid continuous variations through the CMC range instead of mathematically singular changes at an infinitely sharp transition point. Roughly, the larger the micelles being formed at the CMC the sharper will be the "transition." In any case the CMC is not precisely and uniquely defined, and its determination by different experimental methods can be expected to yield somewhat discrepant results.

The present work was inspired by the Yang and Lee analysis of phase transitions in classical statistical mechanics, with emphasis on Ising models.[10] They established for their context the relevance of grand partition function zeros in the complex fugacity plane. We develop here an analogous connection for the complex concentration plane. We believe that a primary value of such an approach for the micelle problem is that it systematically relates measurable colligative properties (such as osmotic pressure) to the size distribution for aggregates. A secondary value is that a precise set of points in the complex concentration plane is now associated with onset of micelle formation, to supplement the somewhat ill-defined "CMC." This latter feature produces an interesting parallelism with quantum theory wherein finite-width resonance states are described in terms of complex energies.[11]

In order to retain maximum simplicity and clarity we have restricted attention in this paper to surfactant solutions that are ideal with respect to the various species of aggregates. The corresponding starting equations appear in Sec. II. We will return to the more general case of interacting species in a later paper. However most of the important concepts and phenomena already arise in the ideal case.

Section III develops our formal theory in the simple case of monodisperse micelles. Section IV then works out an extension of the monodisperse case to a special form of polydispersity. This is followed in Sec. V with a perturbation method for the general case, based on the extended example of Sec. IV. Section VI provides a numerical application of that perturbation method. The final Sec. VII discusses procedures for processing experimental data on osmotic pressures to yield moments of the aggregate size distribution in the CMC region. In addition Sec. VII also mentions several basic issues that must be confronted for future theoretical progress.

II. BASIC RELATIONS

In the ideal solution approximation we can write expressions for osmotic pressure Π and total surfactant number density ρ_t as follows:

$$\beta\Pi = \sum_{j=1}^{\infty} \rho_j \ , \tag{2.1}$$

$$\rho_t = \sum_{j=1}^{\infty} j\rho_j \ . \tag{2.2}$$

[a)] Permanent address: Department of Physical Chemistry, The Hebrew University of Jerusalem, Jerusalem, Israel.

 0021-9606/81/042510-08$01.00

Here β stands for $(k_B T)^{-1}$, and ρ_j is the concentration of j-molecule aggregates. In the case of nonionic surfactants these equations are adequate provided ρ_t is small enough that the volume fraction of surfactant in the solution is much less than unity. A similar restriction also applies to ionic surfactants, but in addition it is necessary to have excess electrolyte present to limit ionization as $\rho_t \to 0$; in this circumstance Π becomes the excess osmotic pressure over that of the supporting electrolyte solution. In both of these cases the ideal solution equations should give a valid description of the critical micelle concentration (CMC) range for many surfactants.

The ρ_j for $j>1$ can be written in terms of ρ_1 by introducing nonnegative association constants K_j:

$$\rho_j = K_j \rho_1^j \ . \tag{2.3}$$

Therefore we have

$$\beta\Pi = \sum_{j=1}^{\infty} K_j \rho_1^j \ , \tag{2.4}$$

$$\rho_t = \sum_{j=1}^{\infty} j K_j \rho_1^j \ . \tag{2.5}$$

Here we have set $K_1 = 1$. Not all sets of K_j will produce a sharp CMC; the theory should eventually tell which sets do.

For the sake of mathematical simplicity in the following analysis we introduce a scaling parameter σ, with dimensions of concentration, by means of which dimensionless quantities can be defined:

$$f = \beta\Pi/\sigma \ , \quad y = \rho_t/\sigma \ , \quad x = \rho_1/\sigma \ , \quad f_j = K_j \sigma^{j-1} \ . \tag{2.6}$$

Hence

$$f(x) = x + \sum_{j>1} f_j x^j \ , \tag{2.7}$$

$$y(x) = x + \sum_{j>1} j f_j x^j \equiv x f'(x) \ . \tag{2.8}$$

Appropriate choices for σ will be specified below.

Although the last equations have been written as though the reduced monomer concentration x were the fundamental variable, that is not in accord with experiment. Instead it is the total concentration of surfactant which is under experimental control. Consequently we wish ultimately to find $f(y)$ and $x(y)$ from Eqs. (2.7) and (2.8).

III. MONODISPERSE MICELLES

It will be helpful to begin by examining the hypothetical example of monodisperse micelles. For this case only one of the association constants will be nonvanishing, namely K_n. By setting

$$\sigma = K_n^{-1/(n-1)} \tag{3.1}$$

we obtain

$$f = x + x^n \ , \tag{3.2}$$

$$y = x + n x^n \ . \tag{3.3}$$

This simple example exhibits characteristic CMC behavior even for modest n values. Figure 1 shows f plotted versus y for $n = 100$, with a clear (but continuous) transition for $y \simeq 0.9$. One finds that increasing n causes this transition to sharpen, and in the limit $n \to \infty$, f develops a discontinuous slope.

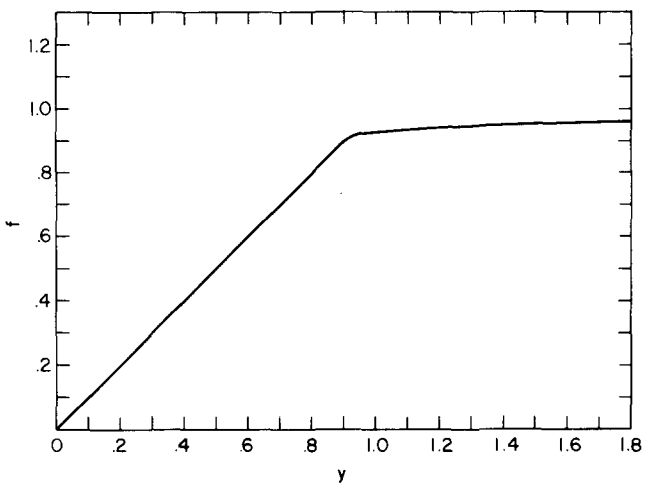

FIG. 1. Reduced osmotic pressure f vs reduced total concentration y for the monodisperse micelle model. In the case shown the aggregate size $n = 100$.

Even though Eq. (3.3) is a relatively simple polynomial it is not possible to write down the inverse function $x(y)$ for arbitrary n. Yet it is this inverse function that is required in order to express the reduced osmotic pressure f in terms of y. Near the origin ($x = 0$) we can iterate (3.3) to find the following power series (convergent for sufficiently small y)

$$x(y) = y - n y^n + n^3 y^{2n-1} - \tfrac{1}{2} n^4 (3n-1) y^{3n-2} + \cdots \ . \tag{3.4}$$

However this inverse function will fail to exist whenever $y'(x)$ vanishes. These singular points lie on a circle in the complex x plane:

$$y'(x) = 0 = 1 + n^2 x^{n-1} \ ,$$

$$x_k = n^{-2/(n-1)} \exp[2\pi i (k + \tfrac{1}{2})/(n-1)] \ , \tag{3.5}$$

where k can take on any $n-1$ successive integer values such as

$$k = 0, 1, 2, \ldots, n-2 \ . \tag{3.6}$$

By substitution in Eq. (3.3) one finds that the corresponding y values also lie on a circle in the complex y plane:

$$y_k \equiv y(x_k) = (n-1) n^{-(n+1)/(n-1)} \exp[2\pi i (k + \tfrac{1}{2})/(n-1)] \ . \tag{3.7}$$

In the vicinity of any x_k in the complex x plane we can write

$$y(x) = y_k + A_k (x - x_k)^2 + O[(x - x_k)^3] \ , \tag{3.8}$$

where we know that the coefficient A_k does not vanish. Consequently the inverse function in this neighborhood must have the following branch-point behavior:

$$x(y) = x_k + A_k^{-1/2} (y - y_k)^{1/2} + O(y - y_k) \ . \tag{3.9}$$

By substitution in Eq. (3.2) we find that f also possesses a branch-point with the same leading-order exponent $\frac{1}{2}$ in the complex y plane:

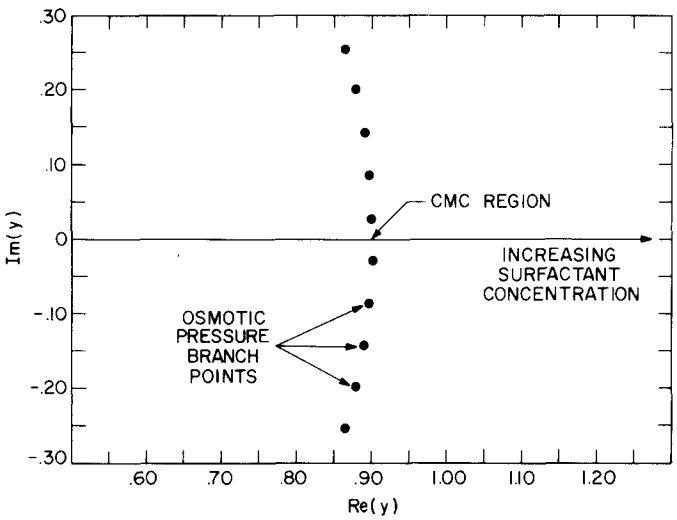

FIG. 2. Branch points in the complex y plane for the monodisperse micelle model, $n = 100$. The critical micelle region occurs where the locus of branch points (a circle for this example) intersects the real concentration axis.

$$f(y) = f(y_k) + (1 - n^{-1}) A_k^{-1/2} (y - y_k)^{1/2} + O(y - y_k) \ . \quad (3.10)$$

For $n = 100$, the y_k, Eq. (3.7), have the common modulus 0.902051.... It is no accident that this radius (of the circle around which the y_k are evenly distributed) is close to the real y value in Fig. 1 at which f is changing its slope most rapidly. As y increases from zero along the positive real axis it eventually must pass from the interior to the exterior of the circle of branch points, slipping between the complex conjugate pair of branch points that most closely straddles the real axis. Figure 2 shows an enlarged view of this region for $n = 100$. Evidently the behavior of $f(y)$ within the branch-point circle is transformed by the passage to a substantially different behavior outside.

The larger n becomes, the closer will be the nearest branch points to the real axis, and the sharper will be the transition. It is this "pinching" of the positive real axis both by complex zeros x_k and by branch points y_k that is analogous to the behavior of grand partition function zeros in the complex fugacity plane elucidated by Yang and Lee.[10] Indeed our variable x is essentially a fugacity.

For large n it is possible to derive simple expressions for the behavior of $f(y)$ in the CMC region. For this purpose we introduce a new variable α by the equation

$$x = r(1 + \alpha/n) \ , \quad (3.11)$$

where

$$r = n^{-2/(n-1)} \quad (3.12)$$

is the modulus of the x_j listed in Eq. (3.5). Then we have

$$y(x) = r(1 + \alpha/n) + nr^n(1 + \alpha/n)^n \sim y(r) + (r/n)[\alpha + \exp(\alpha) - 1] \ . \quad (3.13)$$

Similarly,

$$f(x) = r(1 + \alpha/n) + r^n(1 + \alpha/n)^n \sim f(r) + (r/n)\alpha \ . \quad (3.14)$$

From these expressions it follows that

$$df/dy = (r/n)\, d\alpha/dy = [1 + \exp(\alpha)]^{-1} \ , \quad (3.15)$$

and thereupon

$$d^2f/dy^2 = -(n/r)\{\exp(\alpha)/[1 + \exp(\alpha)]^3\} \ . \quad (3.16)$$

The last four equations for y, f, and the derivatives $f'(y)$ and $f''(y)$ are written in parametric implicit form to be sure, however they allow us to draw some explicit conclusions.

(1) $|f''(y)|$ achieves its maximum value when $\alpha = -\ln 2$, at which point

$$f''(y) = -\tfrac{4}{27} n^{1+2/(n-1)} \ . \quad (3.17)$$

(2) At this point of maximum curvature in the f versus y plot we have

$$f'(y) = \tfrac{2}{3} \quad (3.18)$$

and

$$y = y(r) - (\ln 2 + \tfrac{1}{2})/n^{1+2/(n-1)} \ . \quad (3.19)$$

(3) By comparison the point $y = y(r)$, the point on the real axis marking the radius of the branch-point circle, is located by

$$f''(y) = -\tfrac{1}{8} n^{1+2/(n-1)} \ . \quad (3.20)$$

and

$$f'(y) = \tfrac{1}{2} \ . \quad (3.21)$$

In principle these results could be regarded as necessary conditions that would have to be met by any real surfactant system in order for it to be described accurately by the ideal monodisperse micelle model. Since

$$\frac{df(y)}{dy} = \frac{d\beta\Pi}{d\rho_t} \ , \quad (3.22)$$

a plot of $\beta\Pi$ versus ρ_t should display its maximum downward curvature when its slope is 2/3. If this criterion is met then the next step is to locate the ρ_t value at which the quantity (3.22) equals 1/2; this corresponds to $y(r)$. At this point,

$$yf''(y) = \rho_t \frac{d^2\beta\Pi}{d\rho_t^2} = -(n+1)/8 \ , \quad (3.23)$$

which permits the micelle size to be inferred. Finally, using this latter ρ_t value and the n just obtained the association constant may be calculated:

$$K_n = \left[\frac{n+1}{\rho_t\, n^{1+2/(n-1)}}\right]^{n-1} \ . \quad (3.24)$$

It is unrealistic to expect micelles in real surfactant solutions to be monodisperse. Consequently it is improbable that the necessary conditions just outlined would be satisfied for any given surfactant solution. Nevertheless the simple example just examined is valuable in suggesting how to develop a more general theory.

IV. MODEL POLYDISPERSITY

Before passing on to the most general case it will be useful to examine an extension of the simple model con-

sidered in the preceding section. This extension is defined by the following set of association constants ($\Delta \geq 0$):

$$K_j = 1 \qquad (j=1)\ ,$$
$$= \frac{nn!\,\Delta^{n-j}\,k^{j-1}}{jj!\,(n-j)!\,(1+n^2\Delta^{n-1})} \qquad (2 \leq j \leq n)\ , \tag{4.1}$$
$$= 0 \qquad (n<j)\ .$$

The prior monodisperse model is recovered by setting $\Delta = 0$, in which case

$$K_n = k^{n-1}\ . \tag{4.2}$$

The advantage of the extended form (4.1) is that it continues to lead to clear-cut micelle formation with sizes comparable to n, while it permits polydispersity whose degree is variable and controlled by the parameter Δ. Furthermore this specific form is only moderately more difficult to analyze than its predecessor as the equations below reveal.

By setting $\sigma = k^{-1}$ [Eqs. (2.6)] we find

$$(1+n^2\Delta^{n-1})f(x) = x + nn! \sum_{j=1}^{n} \frac{\Delta^{n-j}x^j}{jj!\,(n-j)!} \tag{4.3}$$

and

$$(1+n^2\Delta^{n-1})y(x) = x + nn! \sum_{j=1}^{n} \frac{\Delta^{n-j}x^j}{j!\,(n-j)!}$$
$$= x + n[(x+\Delta)^n - \Delta^n]\ , \tag{4.4}$$

where we have recognized the binomial coefficients to collapse the sum to the latter form.

Just as in the preceding case $x(y)$ will be singular at points determined by the vanishing of $y'(x)$. The resulting branch points of $f(y)$ will then be associated with the CMC region. From Eq. (4.4) we see that the x_k are determined by

$$0 = 1 + n^2(x+\Delta)^{n-1}\ ,$$
$$x_k = n^{-2/(n-1)} \exp[2\pi i(k+\tfrac{1}{2})/(n-1)] - \Delta\ , \tag{4.5}$$

where k is as before [Eq. (3.6)]. Therefore the only change involved is a shift of the circle of zeros to a new center, at $x = -\Delta$. The corresponding y_k are

$$y_k = y(x_k)$$
$$= (1+n^2\Delta^{n-1})^{-1}[(n-1)\,n^{-1-2/(n-1)}$$
$$\times \exp[2\pi i(k+\tfrac{1}{2})/(n-1)] - \Delta - n\Delta^n]\ . \tag{4.6}$$

Once again the y_k fall on a circle, and like the x_k are shifted in the negative direction. This shift causes the angular aperture of the closest pair of y_k's above and below the real axis to increase, and consequently we might expect the transition to become less sharp as Δ increases at fixed n.

It is possible to show that

$$(1+n^2\Delta^{n-1})f(x) = x + n\sum_{j=1}^{n} \frac{\Delta^{n-j}}{j}[(x+\Delta)^j - \Delta^j]\ ; \tag{4.7}$$

the identity of this expression to that shown in Eq. (4.3) can be demonstrated by expanding the summand and collecting terms of a given x order, along with use of the identity (for $n \geq 1$):

$$\sum_{j=l}^{n} \frac{(j-1)!}{(j-l)!} = \frac{n!}{l(n-l)!}\ . \tag{4.8}$$

We are now in a position to carry out the same type of parametric analysis as before. Set

$$x = r(1+\alpha/n) - \Delta\ , \tag{4.9}$$

where r was defined earlier in Eq. (3.12). By substituting this in Eq. (4.4), we find for large n,

$$y(x) = y(r-\Delta) + (1+n^2\Delta^{n-1})^{-1}(r/n)[\alpha + \exp(\alpha) - 1]\ . \tag{4.10}$$

When the same substitution is used for f in Eq. (4.7) the result is

$$f(x) = f(r-\Delta) + (1+n^2\Delta^{n-1})^{-1}(r/n)$$
$$\times\left\{\alpha + \sum_{j=1}^{n} (\Delta^{n-j}/j)\,n^{[2(n-j)/(n-1)]}[\exp(j\alpha/n) - 1]\right\}. \tag{4.11}$$

Since the $\Delta = 0$ limit corresponds to the case examined in the previous section with just one micelle size, it is clear that for small positive Δ only micelles with sizes close to n will be significant. For larger Δ the micelle size distribution will broaden and move toward smaller mean size.

The subsequent analysis simplifies considerably by confining attention to the small Δ case, for which it is valid to set $n^2\Delta^{n-1}$ to zero, and j/n to unity for the significant j values in the sum in Eq. (4.11). Hence we can write

$$f(x) = f(r-\Delta) + (r/n)\{\alpha + \phi(\Delta,n)[\exp(\alpha) - 1]\}\ , \tag{4.12}$$

where

$$\phi(\Delta,n) = \sum_{k=0}^{n-1} \Delta^k n^{2k/(n-1)}/(n-k)\ . \tag{4.13}$$

From Eqs. (4.10) and (4.12) it is straightforward to show

$$\frac{df}{dy} = \frac{1+\phi\exp(\alpha)}{1+\exp(\alpha)}\ ; \tag{4.14}$$

$$\frac{d^2f}{dy^2} = -\frac{n\exp(\alpha)(1-\phi)}{r[1+\exp(\alpha)]^3}\ . \tag{4.15}$$

Next one can find the α value that yields the maximum downward curvature in a plot of f versus y. From Eq. (4.15) this is found to be

$$\exp(\alpha) = \tfrac{1}{2} + 0(\phi^2)\ . \tag{4.16}$$

The value of the maximum downward curvature then is computed to be

$$f''(y) = -\tfrac{4}{27}\,n^{1+2/(n-1)}[1 - \phi + 0(\phi^2)]\ . \tag{4.17}$$

At this point the slope is

$$f'(y) = \tfrac{2}{3}[1 + \tfrac{1}{2}\phi + 0(\phi^2)]\ . \tag{4.18}$$

In contrast to these last two results we have the following curvature and slope when $\alpha = 0$:

$$f''[y(r-\Delta)] = -\tfrac{1}{8}\,n^{1+2/(n-1)}(1-\phi)\ , \tag{4.19}$$

$$f'[y(r-\Delta)] = \tfrac{1}{2}(1+\phi)\ . \tag{4.20}$$

We are now in a position to see how experimental data

on $\beta\Pi$ versus ρ_t might *in principal* be analyzed in terms of our extended model. First, the ρ_t corresponding to maximum downward curvature in $\beta\Pi(\rho_t)$ must be identified. At this point

$$d\beta\Pi/d\rho_t \simeq \tfrac{2}{3}(1+\tfrac{1}{2}\phi) \ , \tag{4.21}$$

from which ϕ can be evaluated. For consistency, of course, this ϕ must be nonnegative. Next locate the ρ_t for which

$$\frac{d\beta\Pi}{d\rho_t} = \tfrac{1}{2}(1+\phi) \ ; \tag{4.22}$$

at this concentration

$$\rho_t \frac{d^2\beta\Pi}{d\rho_t^2} = -\tfrac{1}{8}[n+1-n^{1+2/(n-1)}\Delta](1-\phi) \ . \tag{4.23}$$

Given that ϕ has already been obtained, which constitutes one relation between n and Δ, Eq. (4.23) provides a second relation between n and Δ which thereupon permits both to be determined individually. Once again consistency requires the resulting Δ to be nonnegative. The last step is to use the latter ρ_t value to give the constant k that appears in Eq. (4.1) for the K_j, specifically

$$k = [n^{-2/(n-1)}(1+n^{-1}) - \Delta]\rho_t^{-1} \ . \tag{4.24}$$

The procedure just outlined constitutes a method for fitting a member of the three-parameter model family to experimental data. The net result of such a fit is an approximation to the exact branch-point locations in the complex concentration plane in terms of a uniform circular distribution.

V. GENERAL AGGREGATION MODEL

Finally we return to the general Eqs. (2.7) and (2.8) for the ideal solution model. The special examples worked out in the two preceding sections indicate what features are likely to be most important. In particular we shall be interested in the location of branch points of $f(y)$ most closely flanking the positive real axis, and in the way those branch points are related to the size distribution of the micellar aggregates.

If a reasonably sharp CMC exists for which finite micelles are formed, then in that CMC range (and above) the size distribution for aggregates is most likely bimodal. That is, the terms in Eq. (2.7) for $f(x)$ and in Eq. (2.8) for $y(x)$ will be significant for the monomer and for those sizes j in the neighborhood of the mean aggregate size. The dispersion in the latter of course depends on the specific set of coefficients f_i under consideration. This bimodality is a characteristic of the example treated in Sec. IV, which suggests that it could serve as the basis for a perturbative analysis of the general case.

The starting point is the equation

$$0 = y'(x) = 1 + \sum_{j>1} j^2 f_j x^{j-1} \ . \tag{5.1}$$

This will not be a polynomial equation if the f_j beyond some order do not identically vanish. But from what has just been said about bimodality the very-high-order terms in Eq. (5.1) should be negligibly small when the variable x corresponds to the CMC range. While an infinite number of terms in Eq. (5.1) will produce an infinite number of zeros in the complex x plane, all but a few will be far removed from the CMC region on the positive real axis and thus may be disregarded.

Define

$$f_j^{(0)}(\Delta, n) = \frac{n^2\Gamma(n)\Delta^{n-j}}{(1+n^2\Delta^{n-1})\, j^2\Gamma(j)\,\Gamma(n-j+1)} \ . \tag{5.2}$$

By referring to Eq. (4.3) above we see that this is just the generic form of the coefficients that appear in the polydisperse model of the preceding Sec. IV. The replacement of factorials by Euler gamma functions affords an extension from discrete n to a continuous variation in this quantity.

In order to assure the success of a perturbative approach it is necessary that the $f_j^{(0)}$ be selected so as to be a close approximation to the f_j. There are three continuous variables at our disposal for this purpose. They are Δ, n, and the scaling parameter σ that was used in Eq. (2.6) to generate reduced variables f, y, x and coefficients f_j for the perturbed problem. We can choose these variables so as to satisfy the following three moment conditions:

$$0 = \sum_{j>1} j(f_j - f_j^{(0)})(r-\Delta)^j \ , \tag{5.3}$$

$$0 = \sum_{j>1} j^2(f_j - f_j^{(0)})(r-\Delta)^j \ , \tag{5.4}$$

$$0 = \sum_{j>1} j^3(f_j - f_j^{(0)})(r-\Delta)^j \ . \tag{5.5}$$

Notice that the first two of these, respectively, cause y and y' at $x = r-\Delta$ to be the same in the perturbed and in the unperturbed versions.

Equation (5.1) may formally be written in the following manner:

$$0 = 1 + \sum_{j>1} j^2[f_j^{(0)} + \lambda(f_j - f_j^{(0)})]x^{j-1} \ , \tag{5.6}$$

where λ is the perturbation parameter, eventually to be set equal to unity. For $\lambda = 0$ the roots were given above in Eq. (4.5) and may now be denoted by $x_k^{(0)}$. It is necessary to compute how these roots shift as λ increases from zero to unity. We can write the formal series,

$$x_k(\lambda) = x_k^{(0)} + \lambda x_k^{(1)} + \lambda^2 x_k^{(2)} + \cdots \ . \tag{5.7}$$

For many applications it should suffice to truncate this series after its second term. By substituting the last equation into Eq. (5.6) and then collecting terms according to order in λ, we find in first order the following result for $x_k^{(1)}$:

$$x_k^{(1)} = R_k x_k^{(0)} \ ,$$
$$R_k = -\left[\sum_{j>1} j^2(f_j - f_j^{(0)})(x_k^{(0)})^{j-1}\right] \Big/ \left[1 + \sum_{j>1} j^3 f_j^{(0)}(x_k^{(0)})^{j-1}\right] . \tag{5.8}$$

The factors R_k will generally be complex numbers.

In the same first order of perturbation it is possible to locate in the complex y plane the images y_k of the roots x_k. One finds

$$y_k = y_k^{(0)} + \lambda y_k^{(1)} + \cdots , \tag{5.9}$$

where

$$y_k^{(0)} = y(x_k^{(0)}) \ ,$$

$$y_k^{(1)} = \sum_{j>1} j(f_j - f_j^{(0)})(x_k^{(0)})^j \ . \tag{5.10}$$

The quantities $y_j^{(0)}$ were given above in Eq. (4.6). In the general case we can expect the perturbation will distort the locus of y_k's into a noncircular shape.

Let $\langle j \rangle$ be the following weighted average over aggregate sizes when $x = r - \Delta$ (which differs from the usual size average):

$$\langle j \rangle = \sum_{j>1} j^3 f_j^{(0)}(r-\Delta)^j \Big/ \sum_{j>1} j^2 f_j^{(0)}(r-\Delta)^j \ . \tag{5.11}$$

Notice that the monomers ($j = 1$) are excluded from these sums. On account of Eqs. (5.4) and (5.5), this expression would be unchanged if the $f_j^{(0)}$ were all replaced by the f_j. Using this average value we can then rearrange Eq. (5.10) for $y_k^{(1)}$ into

$$y_k^{(1)} = \left[\frac{r\exp(i\theta_k) - \Delta}{r-\Delta}\right]^{\langle j\rangle - 1} \sum_{j>1} j(f_j - f_j^{(0)})(r-\Delta)^j$$

$$\times \left\{1 + \left(\frac{r}{r-\Delta}\right)[\exp(i\theta_k) - 1]\right\}^{j - \langle j\rangle + 1} \ , \tag{5.12}$$

where

$$\theta_k = 2\pi(k + \tfrac{1}{2})/(n-1) \ . \tag{5.13}$$

It is reasonable to suppose that the quantities

$$(f_j - f_j^{(0)})(r-\Delta)^j \tag{5.14}$$

appearing in Eq. (5.12) are negligibly small unless j is in the vicinity of $\langle j \rangle$. This, coupled with the fact that most interest centers around small θ_k, justifies use of the following truncated expansion:

$$\left\{1 + \left(\frac{r}{r-\Delta}\right)[\exp(i\theta_k) - 1]\right\}^{j - \langle j\rangle + 1} \simeq 1 + (j - \langle j\rangle + 1)\left(\frac{r}{r-\Delta}\right)$$

$$\times [\exp(i\theta_k) - 1] + \tfrac{1}{2}(j - \langle j\rangle + 1)(j - \langle j\rangle)\left(\frac{r}{r-\Delta}\right)^2$$

$$\times [\exp(i\theta_k) - 1]^2 + \tfrac{1}{6}(j - \langle j\rangle + 1)(j - \langle j\rangle)$$

$$\times (j - \langle j\rangle - 1)\left(\frac{r}{r-\Delta}\right)^3 [\exp(i\theta_k) - 1]^3 \ . \tag{5.15}$$

Consequently Eq. (5.12) reduces to

$$y_k^{(1)} \approx \frac{1}{6}\left(\frac{r}{r-\Delta}\right)^3 [\exp(i\theta_k) - 1]^3 \left[\frac{r\exp(i\theta_k) - \Delta}{r-\Delta}\right]^{\langle j\rangle - 1}$$

$$\times \sum_{j>1} j^4 (f_j - f_j^{(0)})(r-\Delta)^j \ . \tag{5.16}$$

In obtaining this result the moment conditions (5.3)–(5.5) have been used to effect simplifications. Thus we see that displacements of branch point positions in the complex y plane depend upon the fourth moment of the size distribution difference at $x = r - \Delta$.

Starting from Eq. (5.6) with $\lambda = 0$, and then using a procedure analogous to that which produced Eq. (5.16), it is possible to conclude

$$\left[\frac{r\exp(i\theta_k) - \Delta}{r-\Delta}\right]^{\langle j\rangle - 1} = -\left[\frac{1 + n^2\Delta^{n-1}}{1 - n^2\Delta^{n-1}}\right] + O\{[\exp(i\theta_k) - 1]^2\} \ . \tag{5.17}$$

Therefore Eq. (5.16) can be further simplified for those physically relevant branch points near the positive real axis ($|\theta_k|$ small):

$$y_k^{(1)} \approx -\frac{1}{6}\left(\frac{r}{r-\Delta}\right)^3 \left[\frac{1 + n^2\Delta^{n-1}}{1 - n^2\Delta^{n-1}}\right][\exp(i\theta_k) - 1]^3$$

$$\times \sum_{j>1} j^4 (f_j - f_j^{(0)})(r-\Delta)^j \ . \tag{5.18}$$

The key feature of this last Eq. (5.18) is the cubic factor containing θ_k. For those most important y_k near the positive real axis with small phase angles θ_k this factor will be proportional essentially to $-i\theta_k^3$. While this will not change the radius of curvature of the locus at the positive real axis it will produce a cubic aberration. Furthermore it will increase or decrease the spacing of the y_k along the locus according to whether the j sum is, respectively, negative or positive. Along the "backward" direction (θ_k near $\pm\pi$) the effect qualitatively is to compress or to elongate the locus again respectively for negative and for positive j sum.

The fact that the locus is perturbed only in cubic or higher order in the region where it is physically most significant ($\theta_k \simeq 0$) is directly attributable to imposition of the three moment conditions (5.3)–(5.5).

VI. NUMERICAL ILLUSTRATION

In order to test the perturbation approach of the preceding section we now examine a specific example. It is defined by the following association constants

$$\begin{aligned} K_j &= 1 \quad (j = 1) \\ &= k^{j-1} \quad (46 \le j \le 50) \\ &= 0 \quad (\text{all other } j) \ . \end{aligned} \tag{6.1}$$

Here k is a positive constant. After reducing variables in the manner of Eqs. (2.6) we have

$$\begin{aligned} f(x) &= x + \sum_{j=46}^{50} (k\sigma)^{j-1} x^j \ , \\ y(x) &= x + \sum_{j=46}^{50} j(k\sigma)^{j-1} x^j \ . \end{aligned} \tag{6.2}$$

From results displayed in Sec. IV it is straightforward to obtain the following expressions for moments in the unperturbed problem:

$$\sum_{j>1} j f_j^{(0)}(r-\Delta)^j = [n(r^n - \Delta^n) - n^2\Delta^{n-1}(r-\Delta)]/(1 + n^2\Delta^{n-1}) \ , \tag{6.3}$$

$$\sum_{j>1} j^2 f_j^{(0)}(r-\Delta)^j = n^2(r-\Delta)(r^{n-1} - \Delta^{n-1})/(1 + n^2\Delta^{n-1}) \ , \tag{6.4}$$

$$\sum_{j>1} j^3 f_j^{(0)}(r-\Delta)^j = n^2(r-\Delta)[r^{n-1} - \Delta^{n-1} + (n-1)(r-\Delta)r^{n-2}]/$$

$$(1 + n^2\Delta^{n-1}) \ , \tag{6.5}$$

$$\sum_{j>1} j^4 f_j^{(0)}(r-\Delta)^j = n^2(r-\Delta)[r^{n-1} - \Delta^{n-1} + 3(n-1)(r-\Delta)r^{n-2}$$

$$+ (n-1)(n-2)(r-\Delta)^2 r^{n-3}]/(1 + n^2\Delta^{n-1}) \ . \tag{6.6}$$

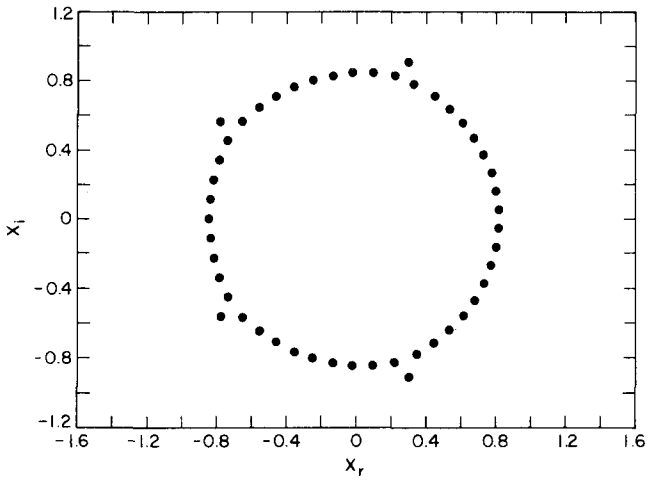

FIG. 3. Zeros of $y'(x)$ in the complex x plane for the aggregation model defined by Eq. (6.1).

These have forms that are suitable for use with noninteger values of n.

For any given value of $k\sigma$ it is elementary to evaluate the corresponding moments for the perturbed case shown in Eq. (6.2). These must then agree, respectively, with Eqs. (6.3), (6.4), and (6.5), according to the starting point of the perturbation procedure shown earlier in Eqs. (5.3), (5.4), and (5.5). Such agreement is possible only for one set of values of $k\sigma$, n, and Δ. We have found numerically that this set is:

$$k\sigma = 1.002\,165\ ,$$
$$n = 49.647\ , \tag{6.7}$$
$$\Delta = 0.034\,297\,9\ .$$

Furthermore the average defined by Eq. (5.11) is found to be

$$\langle j \rangle = 47.688\ . \tag{6.8}$$

Figures 3 and 4 show, respectively, the roots of the 49th degree polynomial for the perturbed problem

$$y'(x) = 0 \tag{6.9}$$

in the complex x plane, and their images in the complex y plane. Although there are four exceptions, most of these points fall on a locus that is nearly circular. In particular this circular shape obtains in the neighborhood of the crossing of the locus with the positive real axis in both planes, which emphasizes the relevance of the perturbative approach.

Using Eq. (6.6) above we next obtain

$$\sum_{j>1} j^4 (f_j - f_j^{(0)})(r-\Delta)^j = 0.045\,547\ . \tag{6.10}$$

It is then possible to go on to calculate the branch point shifts according to formula (5.18). Table I shows some representative results. The first column lists the first few roots y_k of Eq. (6.9) just above the positive real y axis. The second column displays the corresponding $y_k^{(0)}$ for the unperturbed problem. Finally, column three gives the first-order perturbed positions $y_k^{(0)} + y_k^{(1)}$.

TABLE I. Branch point positions in the complex y plane for the association model defined by Eq. (6.1).

k	y_k (exact)	$y_k^{(0)}$	$y_k^{(0)} + y_k^{(1)}$
0	$0.7985 + 0.0539i$	$0.7985 + 0.0539i$	$0.7985 + 0.0539i$
1	$0.7846 + 0.1607i$	$0.7846 + 0.1607i$	$0.7846 + 0.1607i$
2	$0.7571 + 0.2651i$	$0.7571 + 0.2648i$	$0.7570 + 0.2651i$
3	$0.7163 + 0.3654i$	$0.7164 + 0.3645i$	$0.7159 + 0.3651i$
4	$0.6628 + 0.4600i$	$0.6632 + 0.4582i$	$0.6620 + 0.4592i$
5	$0.5974 + 0.5478i$	$0.5984 + 0.5442i$	$0.5958 + 0.5456i$

The message conveyed by Table I is that for the given example the unperturbed positions $y_k^{(0)}$ provide an excellent approximation to the exact y_k, at least in the physically important forward direction. The perturbative corrections for these branch points are negligibly small. In the case of branch points with greater arguments the first order corrections become significant, but apparently ought to be supplemented by higher-order corrections as well.

VII. DISCUSSION

If it is granted that connections exist between (a) critical micelle behavior of the osmotic pressure, (b) branch points in the complex concentration plane, and (c) the aggregate size distribution, the natural question arises about how experimental data for (a) should be processed to yield predictions about (b) and (c). The conclusion suggested by the foregoing is that the polydisperse model developed in Sec. IV above may alone offer the most efficient procedure. It seems to us unlikely that experimental data will be precise enough to warrant a significantly more elaborate treatment.

Section IV has already stated how the three basic parameters (n, Δ, k) are to be inferred. These serve to locate branch-point singularities, and those closely spanning the positive real concentration axis should

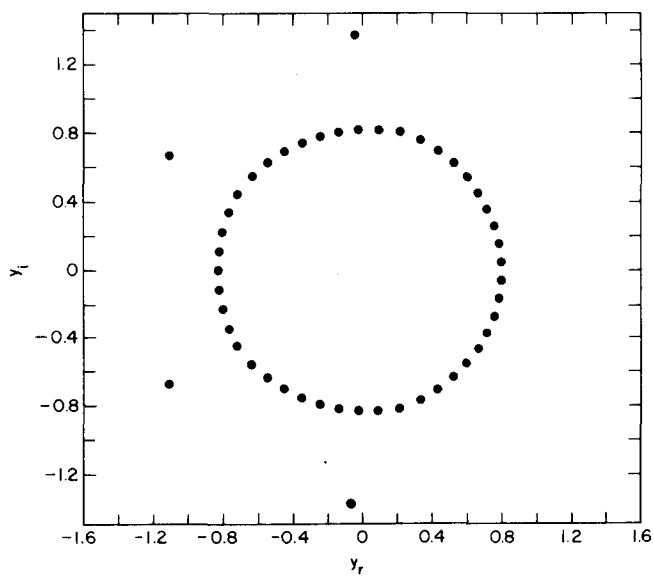

FIG. 4. Branch point locations in the complex y plane for the aggregation model defined by Eq. (6.1).

thereby have been reliably placed. Equations (6.3)–(6.6) subsequently yield four moments of the aggregate size distribution in closed form at the CMC. Other moments could of course also be obtained from the model. In any case the naturally occurring conditions (5.3)–(5.5) in the perturbation theory can be interpreted to mean that the first three moments (6.3)–(6.5) will be particularly robust predictions that are largely immune to the special characteristics of the polydisperse model.

Following the development presented above the primary future demand on the theory is that it be extended to include solution nonideality. This requires accounting specifically for the interactions between aggregates. In principle those interactions can be handled in the statistical mechanical formalism by means of the Ursell–Mayer cluster expansion.[12] Our examination of this problem (to be reported in a later paper) indicates that complex-y-plane branch points are still fundamental to the locating and characterizing of CMC's though in certain special cases their positions can be significantly affected by inter–aggregate interactions. The cluster expansion also appears to be useful for describing the behavior of ionic surfactants in the absence of excess supporting electrolyte.

An important area of future concern must also be derivation of procedures to predict aggregate sizes, structures, and stabilities directly from knowledge of specific surfactant molecular structures and intermolecular forces. While this is no doubt an extremely difficult task to carry out in a purely analytical fashion, computer simulation may have a powerful input to provide. In any case the formalism introduced in this paper should help to connect logically those molecular attributes to the macroscopic regime of measurable solution properties.

Finally, we mention our hope that the present work will stimulate experimentalists to generate precise osmotic pressure data, at closely spaced intervals thoughout the concentration range from zero to well beyond the CMC, to permit a nontrivial test and application of our concepts.

[1]G. C. Kreshek, "Surfactants," in *Water, A Comprehensive Treatise*, edited by F. Franks (Plenum, New York, 1975), Vol. 4.
[2]*Micellization, Solubilization, and Microemulsions*, edited by K. L. Mittal (Plenum, New York, 1977), Vols. 1 and 2.
[3]H. Wennerström and B. Lindman, Phys. Rep. 52, 1 (1979).
[4]C. A. Hoeve and G. C. Benson, J. Phys. Chem. 61, 1149 (1957).
[5]D. C. Poland and H. A. Scheraga, J. Phys. Chem. 69, 2431 (1965).
[6]C. Tanford, J. Phys. Chem. 78, 2469 (1974).
[7]E. Ruckenstein and R. Nagarajan, J. Phys. Chem. 79, 2622 (1975).
[8]R. Nagarajan and E. Ruckenstein, J. Colloid Interface Sci. 60, 221 (1977).
[9]Reference 3, p. 19.
[10]C. N. Yang and T. D. Lee, Phys. Rev. 87, 404 (1952); T. D. Lee and C. N. Yang, Phys. Rev. 87, 410 (1952).
[11]R. G. Newton, *Scattering Theory of Waves and Particles* (McGraw-Hill, New York, 1966).
[12]T. L. Hill, *Statistical Mechanics* (McGraw-Hill, New York, 1956), Chaps. 5 and 6.